Solar Physics
DOI: 10.1007/●●●●●-●●●-●●●-●●●●-●

STEREO SECCHI COR1-A/B Intercalibration at 180° Separation

W. T. Thompson[1] · **J. M. Davila**[2] · **O. C. St. Cyr**[2] · **N. L. Reginald**[3]

Abstract The twin *Solar Terrestrial Relations Observatory (STEREO)* spacecraft reached a separation angle of 180° on 6 February 2011. This provided a unique opportunity to test the intercalibration between the Sun-Earth Connection Coronal and Heliospheric Investigation (SECCHI) telescopes on both spacecraft for areas above the limb. So long as the corona is optically thin, at 180° separation each spacecraft sees the same corona from opposite directions. Thus, the data should appear as mirror images of each other. We report here on the results of the comparison of the images taken by the inner coronagraph (COR1) on the *STEREO Ahead* and *Behind* spacecraft in the hours when the separation was close to 180°. We find that the intensity values seen by the two telescopes agree with each other to a high degree of accuracy. This validates both the radiometric intercalibration between the COR1 telescopes, and the method used to remove instrumental background from the images. The relative error between COR1-A and COR1-B is found to be less than 10^{-9} $B/B_{\odot}$ over most of the field-of-view, growing to a few $\times$ 10^{-9} $B/B_{\odot}$ for the brighter pixels near the edge of the occulter. The primary source of error is the background determination. We also report on the analysis of star observations which show that the absolute radiometric calibration of either COR1 telescope has not changed significantly since launch.

Keywords: Instrumental effects; Corona

1. Introduction

Since the launch of the twin *Solar Terrestrial Relations Observatory (STEREO)* (Kaiser *et al.*, 2008) spacecraft on 26 October 2006, and their subsequent injection into separate heliocentric orbits, the two spacecraft have been slowly drifting apart from Earth in opposite directions at approximately 22.°5 per year, and thus

[1] Adnet Systems Inc., NASA Goddard Space Flight Center
email: William.T.Thompson@nasa.gov
[2] NASA Goddard Space Flight Center
[3] The Catholic University of America, NASA Goddard Space Flight Center

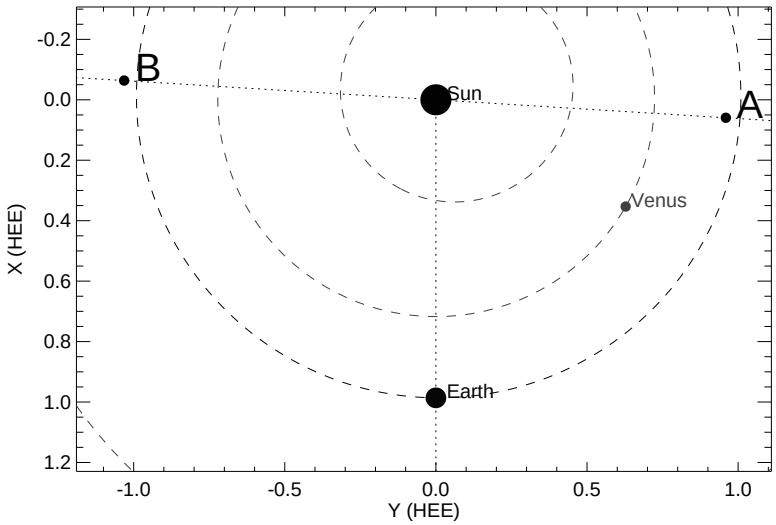

Figure 1. Orbital positions of the *STEREO Ahead (A)* and *Behind (B)* spacecraft at 14:30 UT on 6 February 2011, when the separation angle reached 180°. Positions are plotted in Heliocentric Earth Ecliptic (HEE) coordinates, in Astronomical Units (AU). The orbital paths of the inner planets are also shown, including a small part of the orbit of Mars.

from each other at ∼45° per year. On 6 February 2011, about four years after heliocentric orbital injection, the separation between the two *STEREO* spacecraft reached 180° (Figure 1). One of the major effects of reaching 180° separation is that, when combined with simultaneous images from the Atmospheric Imaging Assembly (AIA) (Lemen *et al.*, 2011) on the *Solar Dynamics Observatory (SDO)*, it allows the first-ever view of the entire Sun (Figure 2). The ability to view the entire Sun will persist for several years, with a hiatus of several months in 2015 when the *STEREO* spacecraft will be out-of-contact on the far side of the Sun. In May 2019, the spacecraft will be once again separated by 180°, when their positions will be essentially reversed from that of Figure 1, with *STEREO Ahead* on the left and *STEREO Behind* on the right. After May 2019 it will no longer be possible to observe the entire Sun; there will be a unobserved area on the solar far side which will grow as the two spacecraft approach Earth.

Another important effect of reaching a separation of 180° is that it serves as a unique opportunity to test the intercalibration above the limb of the sun-pointed telescopes of the Sun-Earth Connection Coronal and Heliospheric Investigation (SECCHI) instrument package (Howard *et al.*, 2008). So long as the corona is optically thin, at 180° separation each spacecraft sees the same corona from opposite directions. Thus, the data should appear as mirror images of each other. We report here on the results of the comparison of the images taken by the inner coronagraph (COR1) on the *STEREO Ahead* (COR1-A) and *Behind* (COR1-B) spacecraft in the hours when the separation was close to 180°.

The importance of deriving an absolute radiometric calibration for the COR1 telescopes cannot be overstated. Absolute brightnesses are needed to convert the

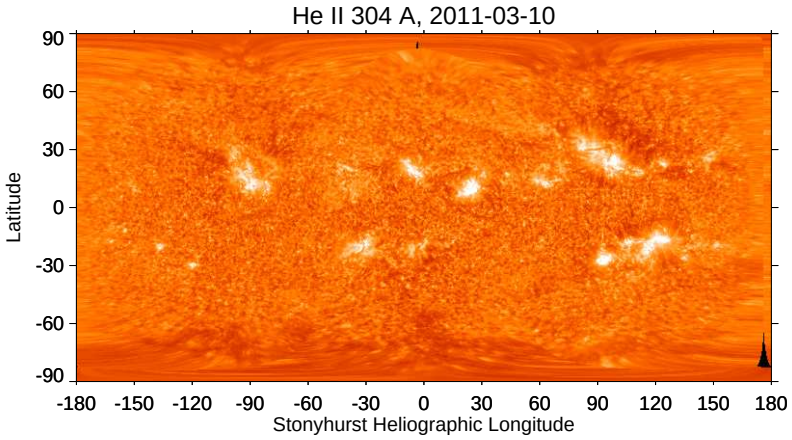

Figure 2. Example synoptic map covering the full solar surface generated from a combination of images in the Helium II emission line at 304 Å from *STEREO-Behind* (left side of map), *SDO* (middle), and *STEREO-Ahead* (right), all taken near 00:00 UT on 10 March 2011.

data into electron densities, and thus derive the physical properties of the solar features under study. One particular area of study where the cross calibration between COR1-A and COR1-B, and with other coronagraphs, is especially important is the tomographic reconstruction of coronal streamers. Kramar *et al.* (2009) apply rotational tomography to COR1-B data to derive electron densities in the streamer belt for Carrington rotations 2058 and 2066, and compare their results to a potential-field source surface model. A more detailed comparison of the same data to an MHD model is presented by Airapetian *et al.* (2011). Butala *et al.* (2010) apply an innovative dynamic tomography technique to both COR1-A and COR1-B data, and compare the results from each spacecraft. Efforts are underway by several groups to derive tomographic reconstructions using simultaneous observations from multiple viewpoints, combining *STEREO* data with those from other coronagraphs. A special campaign (http://soho.nascom.nasa.gov/soc/JOPs/jop224.pdf) was run with *SOHO*/LASCO (Brueckner *et al.*, 1995) from 27 September to 27 October 2009, when the separation angle of both *STEREO* spacecraft with Earth was close to 60°, a geometry particularly favorable for joint tomography.

2. COR1 Calibration

There are several quantities which affect the intercomparison of the COR1-A and COR1-B data. First of all, one needs to know the radiometric calibration of each telescope. This was originally determined using observations of the planet Jupiter in 2007 and 2008 (Thompson and Reginald, 2008). Any changes in the instrumental response over time can be tracked by measuring the brightnesses of the occasional stars which pass through the COR1 field-of-view. A program is in

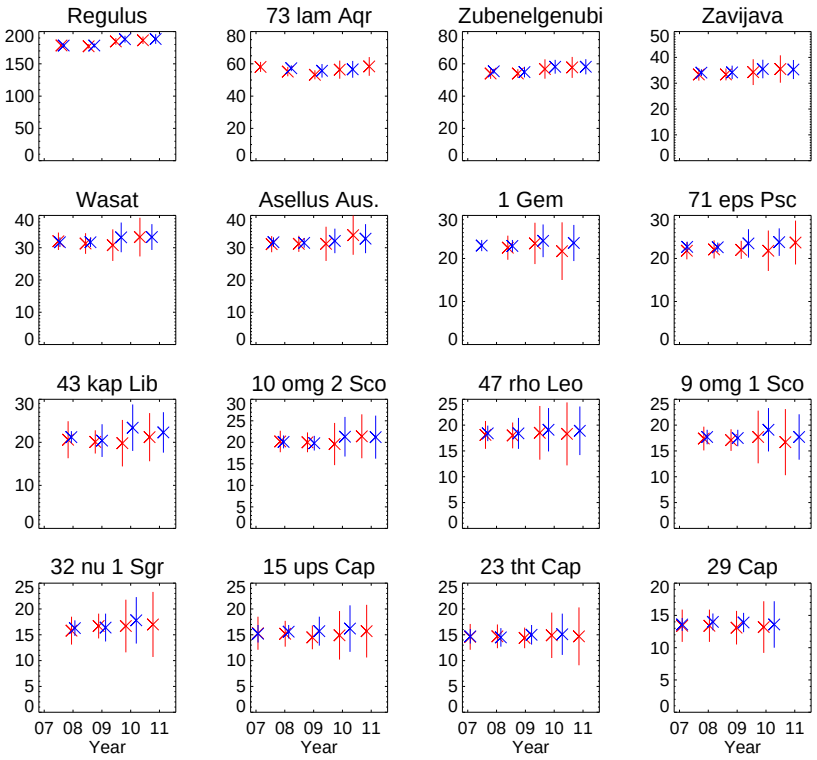

Figure 3. Relative brightnesses as a function of time of 16 stars observed by both the COR1-A (red) and COR1-B telescopes.

place to identify and track stars visible in COR1 data. A total of 55 separate stars have been identified as appearing in either COR1-A or COR1-B images, with most appearing in both telescopes. Figure 3 shows the observed brightnesses of 16 well-observed stars. It's quite evident that there are no consistent trends in the star brightnesses, and that the COR1-A and COR1-B measurements agree quite well. The data are in nominal units of $10^{-9}\ B/B_{\odot}$; however, these units are not meaningful when applied to stars. On 19 April 2009, the COR1 binning on both spacecraft was increased to bring down 512×512 images instead of the previous 1024×1024 images. Star brightnesses after this date are adjusted by a factor of 4 to take the different binning size into account. Some of the star brightnesses (e.g. Regulus) show a slight increase (4–6%) after the change in binning, as well as an increase in the statistical uncertainties for all stars.

It's also important to know the precise telescope pointing to be able to do a pixel-by-pixel comparision between the two telescopes. The pointing of COR1-B was established from observations of the Moon as it transited the Sun on 24 February 2007, while the same was done for COR1-A using observations of the bright star λ-Aquarii a few days later (Thompson and Reginald, 2008). The same star observations discussed above for monitoring the radiometric calibration are also used to track the stability of the pointing calibration.

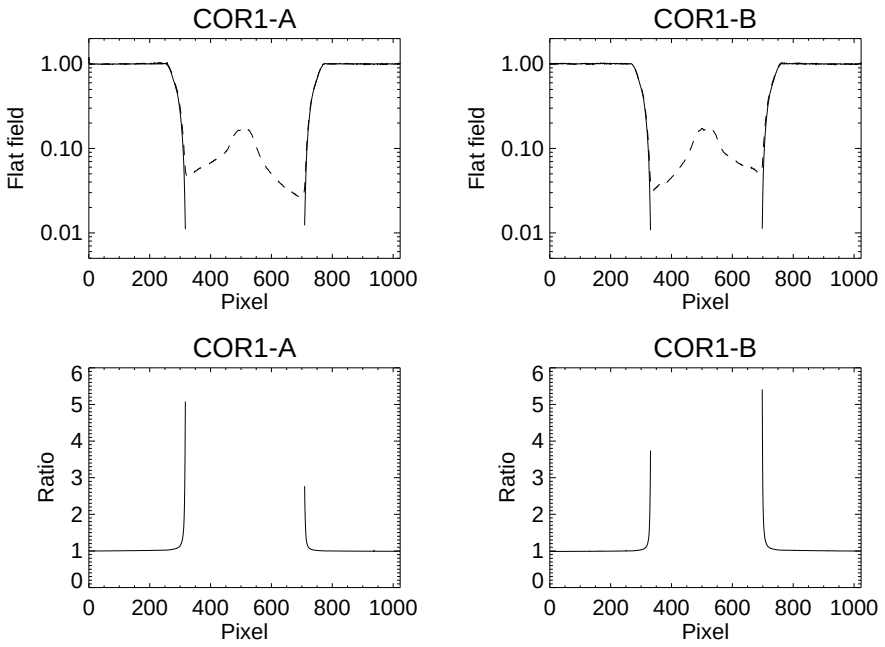

Figure 4. Demonstration of the improvement Top panels: Traces through the center of the COR1 instrument flat fields as implmented in 2007 (dashed) and 2009 (solid). The July 2009 flat field corrections cut off below a factor 0.01 to avoid runaway data within the occulter shadow. Bottom panels: Ratios of data from top panels, showing the substantial improvement at the edge of the occulter, with little change elsewhere.

Another important quantity is the instrumental flat field. The COR1 flat field is derived from observations using an opal window built into the aperture door (Thompson and Reginald, 2008). Most of the COR1 field-of-view is unvignetted, and the flat field in these regions is very close to unity. However, the areas close to the edge of the occulter or field stop are strongly vignetted, and a substantial correction factor needs to be applied in these regions. In July 2009 the data used to derive the COR1 flat field images were reanalyzed to take into account a small amount of scattered light which appears in the door-closed images. This resulted in signficant changes to the flat field correction in the most occulted regions, but little change elsewhere, as demonstrated in Figure 4. With the 2007 version of the flat field, the maximum correction was a factor of $\sim$20 in the most vignetted regions. The new flat fields increases this correction to a maximum of 100. Corrections larger than 100 are not made to avoid data runaway in the totally occulted regions. These new flat field corrections were implemented in *SolarSoft* (Freeland and Handy, 1998) on 27 July 2009.

Finally, one must also be able to dependably remove the instrumental background. Since the COR1 front objective is exposed to direct sunlight, the data are dominated by scattered light which needs to be removed to isolate the actual signal for the K-corona. Thompson *et al.* (2010) describes the method used to

derive the time-dependent instrumental backgrounds, based on a combination of monthly minima and calibration roll data.

The 180° separation of the spacecraft on 6 February 2011 marks the first time that the data from the COR1-A and COR1-B telescopes can be directly compared since early 2007 when both spacecraft were still close to Earth. The question naturally arises whether the calibration has been maintained in the intervening four years. We test this below by applying the standard SECCHI analysis software, which incorporates all of the above calibration factors, to data from both COR1 telescopes and see how well they compare.

3. Data Reduction

The two *STEREO* spacecraft passed the 180° separation mark in ecliptic longitude at 17:08 UT on 6 February 2011. However, this way of measuring the separation does not take into account the slight inclination of the spacecraft orbits to the ecliptic plane. A more precise treatment uses the three-dimensional heliocentric separation angle, which by definition is always $\leq 180°$. For *STEREO*, the maximum separation was 179.°7, which occurred a few hours earlier at 14:30 UT. This small difference from exactly 180° is not enough to be significant.

The standard COR1 observation takes a sequence of images with the internal polarizer set at 0°, 120°, and 240°. We selected a four hour window between 12:30 and 16:30 UT, centered on the time of maximum separation at 14:30 UT. Since the COR1 cadence was 5 minutes, this gives us a toal of 49 polarizer sequences to analyze for both spacecraft. We first processed the data through the *SolarSoft* routine `SECCHI_PREP`, using the keywords `/CALROLL` to select the background images based on a combination of calibration roll and monthly minima, and `/INTERPOLATE` to interpolate the backgrounds which are calculated every 10 days. Special calibration rolls were performed on both spacecraft on dates close to 6 February 2011 specifically to assist in *STEREO-A/B* cross-calibration. The calibration roll for *STEREO-Ahead* was performed on 1 February, and the corresponding roll for *Behind* was performed on 8 February. It was fortunate that these rolls were performed when they were, because the COR1-A background jumped up suddenly on 11 February 2011 when a small piece of dust landed on the front objective. Thus, only data prior to this event can be used to derive backgrounds to apply to the data taken on 6 February.

After processing through `SECCHI_PREP`, the data taken at each polarizer position were averaged separately to reduce the noise, and the resulting three images were analyzed to derive the total brightness (B) and polarized brightness (pB). This was done using the *SolarSoft* routine `COR1_FITPOL` which suppresses spurious pB signals due to noise compared to the method implemented in `SECCHI_PREP` (Thompson *et al.*, 2010).

Figure 5 shows the resulting B and pB images for both spacecraft. Theoretically, the COR1-A and COR1-B data should be mirror images of each other. This is more true for pB than for B. Since pB is determined from differences between the images at the various polarization positions, it is less sensitive than B to small errors in the background subtraction. The arrow points to a region

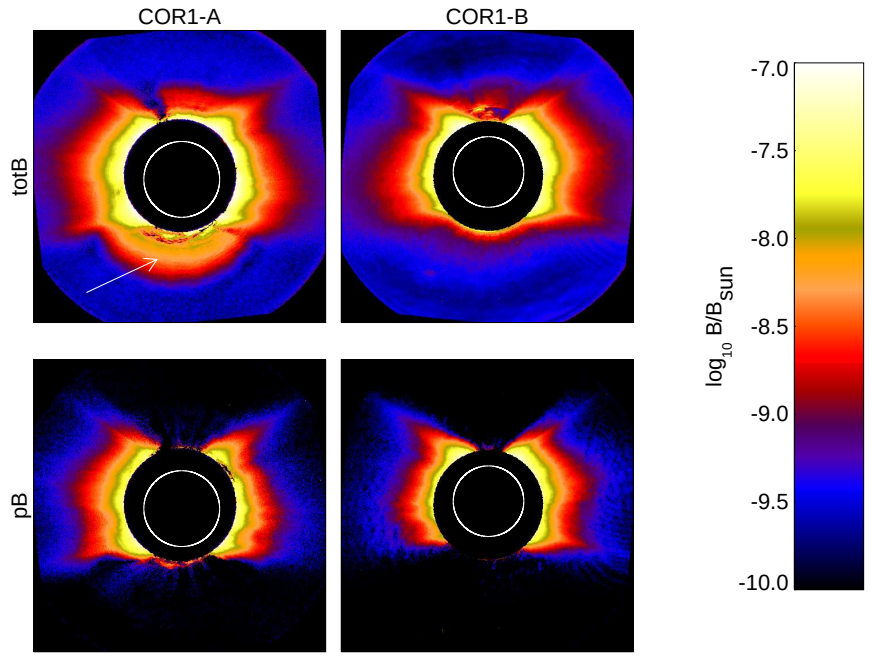

Figure 5. Total brightness (top panels) and polarized brightness (bottom panels) images for COR1-A and COR1-B averaged over four hours centered on the time of maximum separation at 14:30 UT on 6 February 2011. The white circles represent the position of the Sun behind the occulter. The arrow marks a region where there is a known problem in the COR1-A unpolarized background subtraction.

where the COR1-A background has significant temporal evolution, and thus is problematic when deriving B (Thompson *et al.*, 2010). The strength of this feature may be aggravated by the fact that the COR1-A background changed suddenly on 11 February, making the interpolation of the background somewhat less reliable. There is also a region near the north pole where the COR1-B B image is distorted by small features on the field lens (Thompson and Reginald, 2008). These features do not appear in pB; therefore, we will concentrate on comparing pB from COR1-A and COR1-B in the remainder of the analysis.

Figure 6 shows the pB data from Figure 5 resampled into a polar grid of solar radii versus position angle. This facilitates a pixel-by-pixel comparison between the telescopes. Since theory predicts that the COR1-B image should be a mirror-image of that of COR1-A, this has been taken into account by reversing the COR1-B position angle. Because the Sun is not centered behind the COR1 occulters, the occulter edge for each spacecraft appears as a sinusoidal shape in Figure 6.

Since the data in Figure 6 are co-aligned, one can directly compare the COR1-A brightnesses with those from COR1-B. Figure 7 shows the correspondence between the two telescopes for all pixels above a brightness of 10^{-10} $B/B_{\odot}$. It's quite evident that the brightnesses are well correlated. For more than 88% of the points in Figure 7, the brightness difference between the two COR1 telescopes

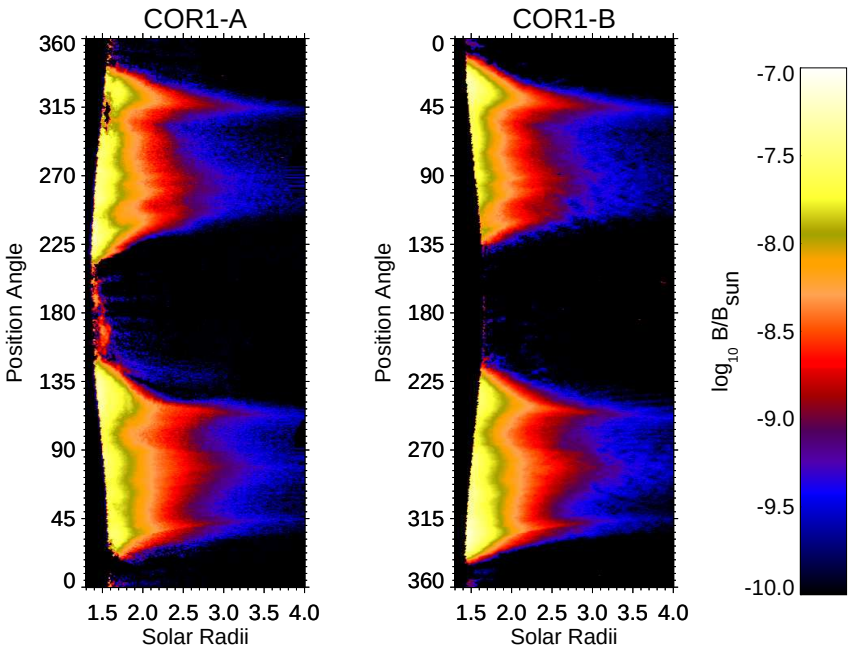

Figure 6. Polarized brightness data from Figure 5 resampled into a polar representation. The position angle for COR1-B has been reversed to reflect the expected mirror-image nature of the data.

is less than 10^{-9} $B/B_{\odot}$; brighter pixels near the occulter edge have differences of a few $\times$ 10^{-9} $B/B_{\odot}$.

A more direct comparison of the COR1-A and COR1-B data appears in Figure 8 which shows azimuthal traces of the brightnesses for several heights from 1.7–3.5 $R_{\odot}$, averaged between the limits shown in the figure. As in Figure 6, the COR1-B position angles are reversed to allow comparison with COR1-A. The same coronal features are clearly evident in both telescopes at all heights. The background determination method forces the estimated brightnesses in the polar coronal hole regions to be close to zero (Thompson *et al.*, 2010); this is a known limitation of the COR1 background processing.

Figure 9 shows radial scans along several representative streamers, averaged over the range of position angles shown in the figure. The radial profiles of each streamer matches well in both telescopes. The largest differences of a few $\times$ 10^{-9} $B/B_{\odot}$ are seen in the streamer at 240°, as can also be seen in Figure 8. Some differences between COR1-A and COR1-B can also be seen at large radial distances for the streamer at 320°; however, the brightnesses are quite faint in this part of the streamer.

4. Conclusions

The 180° separation between the two *STEREO* spacecraft on 6 February 2011 afforded a unique opportunity to check the cross calibration between the tele-

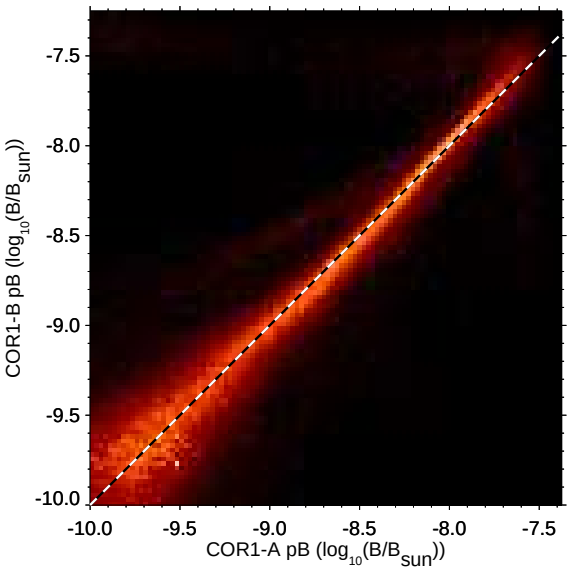

Figure 7. Scatter map between COR1-A and COR1-B pB values. The brightness is proportional to the number of pixels in that bin. The dashed line is for a theoretical one-to-one relationship.

scopes on each spacecraft. The previous time that such a direct comparison was possible was in early 2007 when both spacecraft were still close to Earth. The excellent agreement between COR1-A and COR1-B at 180° separation demonstrates that the relative radiometric calibration has not changed in the intervening four years. Monitoring of star brightnesses also show no change in the radiometric calibration of either COR1 telescope, and rules out the remote possibility that the calibrations of the two telescopes were changing in unison.

The COR1 instrumental backgrounds are quite different between the *STEREO-Ahead* and *Behind* spacecraft. The backgrounds also change with time due to a number of causes. First, there is a periodic background change due to the changing orbital distance. Since the orbit of *STEREO-Behind* has a higher eccentricity than that of *STEREO-Ahead*, this effect is more noticeable for COR1-B than for COR1-A. Second, there are also sporadic changes due to new particles adhering to the objective lens of each telescope. Since the COR1 objectives are exposed to full sunlight, even small particles can have a significant effect on the instrumental background. Finally, there is a slowly growing feature in the COR1-A background which is not yet understood (Figure 5); fortunately, this feature is unpolarized, and has no effect on pB.

A previous publication (Thompson *et al.*, 2010) outlined the procedure used to track the changes in the COR1 backgrounds. The excellent agreement between COR1-A and COR1-B at 180° separation also validates the method used to derive the instrumental backgrounds. The method is known to overcorrect in the polar coronal hole regions, but the present work demonstrates that streamer brightnesses are quite robust. The relative error between COR1-A and COR1-B

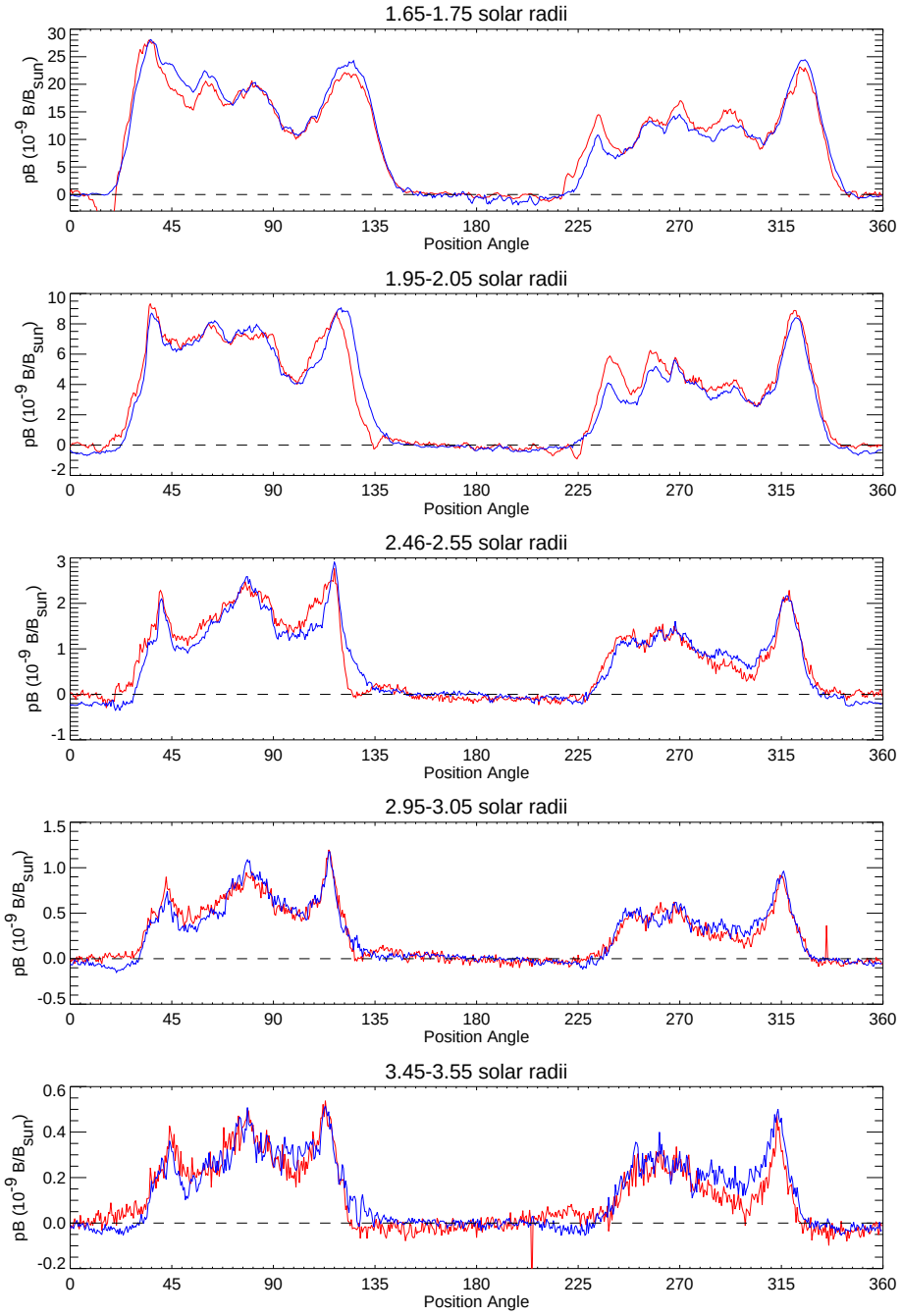

Figure 8. Polarized brightness values as a function of position angle for selected heights for COR1-A (red) and COR1-B (blue). The position angles for COR1-B are reversed.

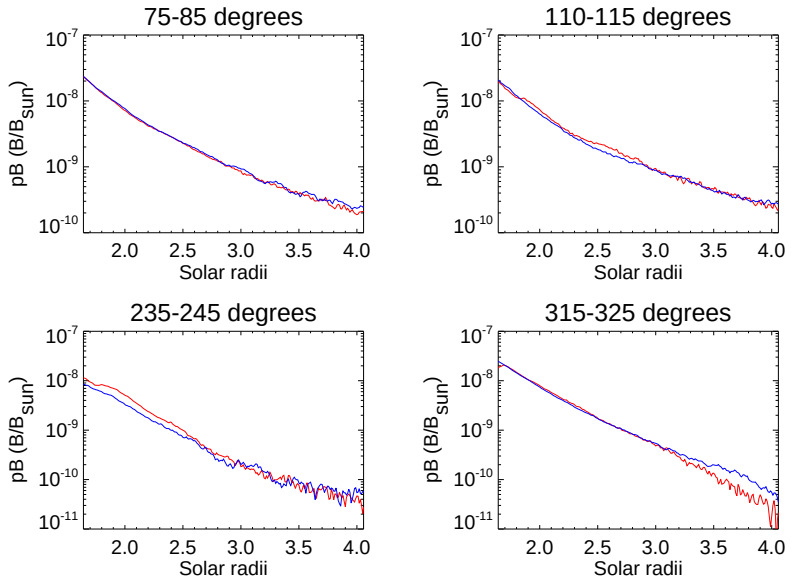

Figure 9. Polarized brightness values as a function of elevation along several representative streamers for COR1-A (red) and COR1-B (blue). The position angles for COR1-B are reversed.

is found to be less than 10^{-9} $B/B_{\odot}$ over most of the field-of-view, growing to a few $\times$ 10^{-9} $B/B_{\odot}$ for the brighter pixels near the edge of the occulter. The primary source of error is in the time-dependent background determination, which cancels out in running-difference or base-difference images.

References

Airapetian, V., Ofman, L., Sittler, E.C., Kramar, M.: 2011, Probing the thermodynamics and kinematics of solar coronal streamers. *Astrophys. J.* **728**, 67 – 76.

Brueckner, G.E., Howard, R.A., Koomen, M.J., Korendyke, C.M., Michels, D.J., Moses, J.D., Socker, D.G., Dere, K.P., Lamy, P.L., Llebaria, A., Bout, M.V., Schwenn, R., Simnett, G.M., Bedford, D.K., Eyles, C.J.: 1995, The Large Angle Spectroscopic Coronagraph (LASCO). *Solar Physics* **162**, 357 – 402. doi:10.1007/BF00733434.

Butala, M.D., Hewett, R.J., Frazin, R.A., Kamaladabadi, F.: 2010, Dynamic three-dimensional tomography of the solar corona. *Solar Phys.* **262**, 495 – 509.

Freeland, S.L., Handy, B.N.: 1998, Data analysis with the SolarSoft system. *Solar Physics* **182**, 497 – 500.

Howard, R.A., Moses, J.D., Vourlidas, A., Newmark, J.S., Socker, D.G., Plunkett, S.P., Korendyke, C.M., Cook, J.W., Hurley, A., Davila, J.M., Thompson, W.T., Cyr, O.C.S., Mentzell, E., Mehalick, K., Lemen, J.R., Wuelser, J.P., Duncan, D.W., Tarbell, T.D., Wolfson, C.J., Moore, A., Harrison, R.A., Waltham, N.R., Lang, J., Davis, C.J., Eyles, C.J., Mapson-Menard, H., Simnett, G.M., Halain, J.P., Defise, J.M., Mazy, E., Rochus, P., Mercier, R., Ravet, M.F., Delmotte, F., Auchere, F., Delaboudiniere, J.P., Bothmer, V., Deutsch, W., Wang, D., Rich, N., Cooper, S., Stephens, V., Maahs, G., Baugh, R., Mcmullin, D.: 2008, Sun Earth Connection Coronal and Heliospheric Investigation (SECCHI). *Space Sci. Rev.* **136**, 67 – 115.

Kaiser, M.L., Kucera, T.A., Davila, J.M., St. Cyr, O.C., Guhathakurta, M., Christian, E.: 2008, The STEREO mission: An introduction. *Space Sci. Rev.* **136**, 5 – 16.

Kramar, M., Jones, S., Davila, J., Inhester, B., Mierla, M.: 2009, On the tomographic reconstruction of the 3D electron density for the solar corona from STEREO COR1 data. *Solar Phys.* **259**, 109 – 121.

Lemen, J.R., Title, A.M., Akin, D.J., Boerner, P.F., Chou, C., Drake, J.F., Duncan, D.W., Edwards, C.G., Friedlaender, F.M., Heyman, G.F., Hurlburt, N.E., Katz, N.L., Kushner, G.D., Levay, M., Lindgren, R.W., Mathur, D.P., McFeaters, E.L., Mitchell, S., Rehse, R.A., Schrijver, C.J., Springer1, L.A., Stern, R.A., Tarbell, T.D., Wuelser, J.-P., Wolfson, C.J., Yanari, C., Bookbinder, J.A., Cheimets, P.N., Caldwell, D., Deluca, E.E., Gates, R., Golub, L., Park, S., Podgorski, W.A., Gummin, M.A., Smith, P., Auker, G., Jerram, P., Pool, P., Soufli, R., Windt, D.L., Beardsley, S., Clapp, M., Lang, J., Waltham, N.: 2011, The Atmospheric Imaging Assembly on the Solar Dynamics Observatory. *Solar Phys.* submitted.

Thompson, W.T., Reginald, N.L.: 2008, The radiometric and pointing calibration of SECCHI COR1 on STEREO. *Solar Phys.* **250**, 443 – 454.

Thompson, W.T., Wei, K., Burkepile, J.T., Davila, J.M., Cyr, O.C.S.: 2010, Background subtraction for the SECCHI/COR1 telescope aboard STEREO. *Solar Phys.* **262**, 213 – 231.